Int. J. Electrochem. Sci., 16 **(2021)** Article Number: 211020, doi: 10.20964/2021.10.17

International Journal of
ELECTROCHEMICAL
SCIENCE
www.electrochemsci.org

Enhanced Visible Light-driven Photocatalytic Activities of Ag_3PO_4 Modified Electrochemically Anodized TiO_2 Nanotube Arrays

Guangxing Ping[1,2], *Xinyan Wang*[2], *Da Chen*[3,*], *Kangying Shu*[3] *Changsheng Li*[1,*]

[1] School of Material Science and Engineering, Jiangsu University, Zhenjiang, Jiangsu 212013, China
[2] College of Sciences, China Jiliang University, Hangzhou, Zhejiang 310018, China
[3] College of Materials and Chemistry, China Jiliang University, Hangzhou, Zhejiang 310018, China
[*]E-mail: dchen_80@hotmail.com ; lichangsheng@ujs.edu.cn

Received: 1 June 2021 / *Accepted:* 26 July 2021 / *Published:* 10 September 2021

In this work, the Ag_3PO_4/TiO_2 nanotube arrays (TNTAs) composite photocatalysts were successfully prepared by a facile chemical impregnation method, and their photocatalytic properties were investigated. It was found that the TNTAs sample, which was prepared by electrochemical anodization, consisted of a highly ordered array of nanotubes with a diameter of about 110 ± 10 nm. For the Ag_3PO_4/TNTAs sample, Ag_3PO_4 nanoparticles (ca. 2~8 nm) were uniformly distributed on the surface of TNTAs. The TNTAs sample mainly absorbed ultraviolet light and rarely visible light. In contrast, the Ag_3PO_4/TNTAs sample absorbed much stronger visible light while maintaining ultraviolet light absorption. More importantly, the visible light photocatalytic activity of Ag_3PO_4/TNTAs for rhodamine B (RhB) degradation was much better than that of TNTAs, and the photodegradation rate constant of Ag_3PO_4/TNTAs was about 2.6 times that of TNTAs. The improved photocatalytic activity of Ag_3PO_4/TNTAs could be attributed to the following two aspects: (1) the loading of Ag_3PO_4 could improve the visible light absorption performance and spectral utilization efficiency of TNTAs; and (2) the heterojunctions formed between Ag_3PO_4 and TNTAs could be beneficial for the separation and transfer of photogenerated charges, which would greatly improve the photocatalytic performance of TNTAs.

Keywords: TiO_2 nanotube arrays (TNTAs); Ag_3PO_4 nanoparticles; Electrochemical anodization; Composite photocatalysts; Photocatalytic activities

1. INTRODUCTION

Modern industry has severely polluted the water resources on which we depend. Particularly, organic pollutants in the wastewater pose a great threat to the health of humans and aquatic organisms due to their high toxicity, carcinogenicity and mutagenicity [1-3]. Among the reported solutions to

remove organic pollutants in water, photocatalysis has attracted much attention [4-7]. As the most widely used semiconductor photocatalyst, TiO_2 has received great attention in solving environmental pollution problems because of its relatively good photocatalytic activity, low price, no toxicity, good stability, and mild reaction conditions as well as the ability to completely mineralize the organic pollutants into CO_2 and H_2O [6, 8, 9]. Compared with other forms of nano TiO_2 materials, TiO_2 nanotube arrays (TNTAs), which were firstly obtained by electrochemical anodization in 2001 [10], has obvious advantages in the following aspects. Firstly, due to their unique one-dimensional (1D) nanotube structure, TNTAs possess highly ordered pores, high specific surface area and anisotropic properties, thus exhibiting relatively good photoelectrochemical performances. Secondly, TNTAs are grown on the surface of titanium sheet, and the firm connection between them improves the structural stability and ease of use of TNTAs, and also facilitates the reuse of TNTAs. Lastly, more important is the well-ordered tubular nanostructure of TNTAs to offer much more spaces inside and outside the tubes that can be filled with other active substances [11-15], and thereafter realize the modification of TNTAs. In view of these advantages, the TNTAs may always predominate over TiO_2 nanoparticles in the fields of photocatalysis, sensing, solar cells and so on [16]. However, the major drawbacks inherent in TiO_2, i.e., poor visible light absorption induced by its wide band-gap and easy recombination of photogenerated charges [17], greatly restrict the practical applications of TNTAs. To overcome these obstacles, it is necessary to modify TNTAs.

On the other hand, Ag_3PO_4, as a novel photocatalyst discovered by Ye's group in 2010 [18], possesses good visible light absorption abilities and excellent visible light photocatalytic activities. Actually, the photocatalytic degradation rate of organic dyes over Ag_3PO_4 is more than ten times those of other visible light photocatalysts (e.g., $BiVO_4$ and $TiO_{2-x}N_x$) [18-20], and thus Ag_3PO_4 has attracted much attention in the field of photocatalysis. In spite of its extremely high photocatalytic activity, the poor structural stability of Ag_3PO_4 as a result from the photocorrosion in the photocatalytic system inevitably becomes a major bottleneck for its application [21, 22].

In view of the respective advantages of Ag_3PO_4 and TNTAs, herein, Ag_3PO_4 nanoparticles were deposited onto the surface of TNTAs to form the composite photocatalyst of Ag_3PO_4/TNTAs. The obtained Ag_3PO_4/TNTAs composites were then characterized by using various characterization techniques, and their photocatalytic performances were also evaluated by photodegradation of rhodamine B (RhB). It is expected that the coupling of Ag_3PO_4 nanoparticles with TNTAs would significantly improve the photocatalytic activity of TNTAs.

2. EXPERIMENT

2.1 Preparation of Ag_3PO_4/TNTAs

TNTAs were prepared by electrochemical anodization of Ti foil according to our previous work [13]. The deposition of Ag_3PO_4 nanoparticles onto the TNTAs was obtained through a chemical impregnation method. Typically, the prepared TNTAs were firstly immersed into solution A consisting of 0.03 mol of $AgNO_3$, 0.06 mol of oleylamine and 90 mL of toluene for 20 min, and then transferred to solution B consisting of 0.03 mol of H_3PO_4 and 30 mL of ethanol and kept for 5 min. This procedure

was repeated for 5 times to obtain the Ag_3PO_4/TNTAs composite. After the impregnation process, the obtained Ag_3PO_4/TNTAs composite was ultrasonically rinsed in the ethanol solution of 0.02 M NH_4OH for 5 min to remove the residual oleylamine. The resulting product was finally dried at 60 ^oC in vacuum for 2 h.

2.2 Materials characterization

The crystal structures of the obtained samples were characterized by X-ray diffraction (XRD, BRUKER, D2 PHASER, Germany). The morphological features of the samples were examined by field emission scanning electron microscopy (FESEM, HITACHI SU 8010, Japan), and the corresponding microstructures were further characterized by transmission electron microscopy (TEM, JEOL JEM-2100, Japan). The UV–vis spectra of the prepared samples were determined by a UV–vis spectrometer (UV–vis-NIR Spectrophotometer, SHIMADZU, UV-3600, Japan) equipped with integrating sphere accessory.

2.3 Photocatalytic evaluation

The photocatalytic activities of the prepared samples were evaluated by photocatalytic degradation of RhB aqueous solution (5 mg L^{-1}) under visible light irradiation. For the photocatalytic measurement, the obtained TNTAs or Ag_3PO_4/TNTAs photocatalyst was placed in a quartz-glass vessel containing RhB aqueous solution, which was exposed to the visible light ($\lambda \geq 420$ nm) irradiation with an average intensity of 20 mW cm^{-2} produced by a 100-W Xenon lamp assembled with an optical filter. The vessel was placed at a distance of 40 cm from the light source, and kept in the dark for 30 min to achieve an adsorption/desorption equilibrium on the samples before the light irradiation. During the photocatalytic process, the absorbance of the RhB solution was measured every 20 minutes at a wavelength of 554 nm (the maximum absorption band) using a UV–vis spectrophotometer (Puxi, TU-1901, China). The test data were recorded and analyzed to determine the photocatalytic properties of the product.

3. RESULTS AND DISCUSSION

3.1 Characterizations of Ag_3PO_4/TNTAs

Figure 1 shows the XRD patterns of the prepared TNTAs and Ag_3PO_4/TNTAs samples. As seen, the TNTAs sample exhibited obvious characteristic diffraction peaks corresponding to the crystal structure of anatase (JCPDS No. 21-1272), while other characteristic diffraction peaks could be attributed to the crystal structure of Ti metal phase (JCPDS No. 44-1294) on the Ti substrate [14, 23]. As a comparison, the XRD diffraction pattern of the Ag_3PO_4/TNTAs sample was nearly unchanged, indicating that the deposition of Ag_3PO_4 nanoparticles would not change the crystal structure of TNTAs. Meanwhile, the characteristic diffraction peaks of Ag_3PO_4 were not observed in the XRD pattern of

Ag_3PO_4/TNTAs, which could be due to the low loading amount of Ag_3PO_4 nanoparticles in the composite. A similar phenomenon has also been observed in the Ag_3PO_4-modifed composite photocatalysts [24].

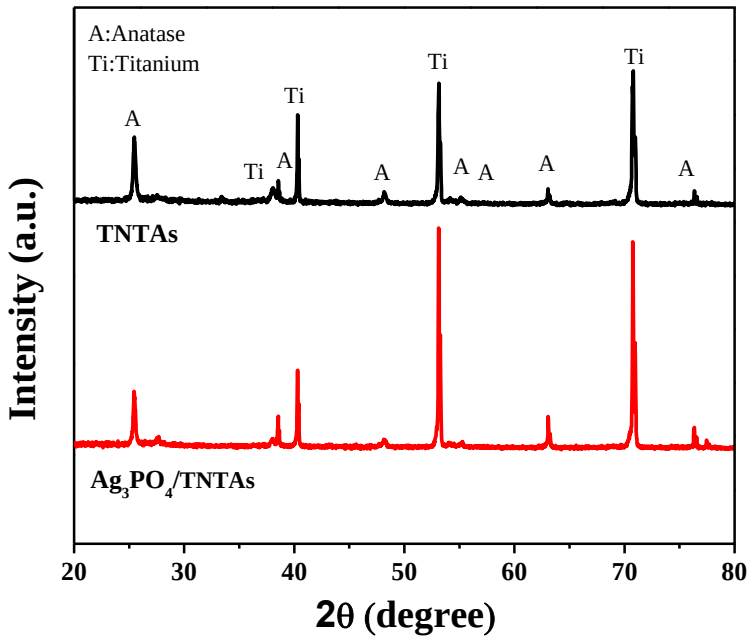

Figure 1. XRD patterns of the prepared TNTAs and Ag_3PO_4/TNTAs samples

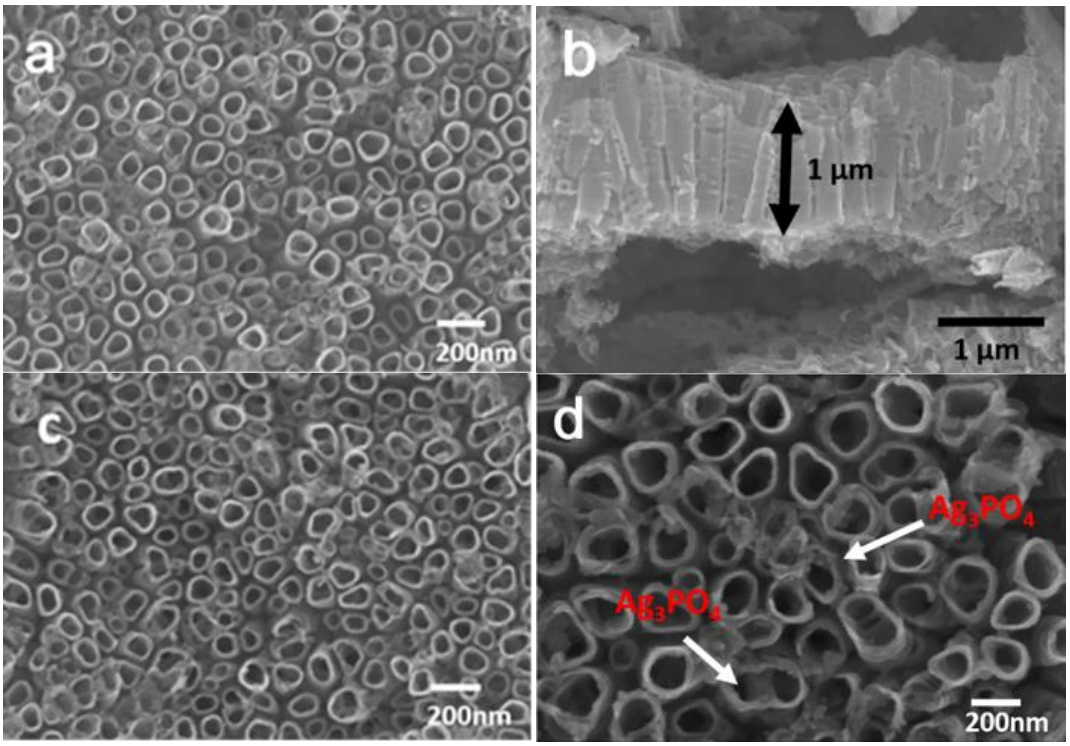

Figure 2. FESEM images of the prepared TNTAs ((a) top view, (b) cross-sectional view) and Ag_3PO_4/TNTAs ((c) low magnification, (d) high magnification).

Figure 2 shows the FESEM images of the prepared TNTAs and Ag_3PO_4/TNTAs samples. As shown, the TNTAs sample possessed an obvious nanotube array structure (Figure 2(a)), in which the TNTAs surface was relatively flat and the nanotubes were uniformly distributed with a tube diameter of about 110 ± 10 nm and a tube wall thickness of about 15 nm. This is consistent with the typical structural and morphological features of the electrochemically anodized TNTAs reported in the literature [25-27]. From the cross-sectional FESEM image of the TNTAs (Figure 2(b)), the length of the nanotube arrays was estimated to be about 1 μm. For the Ag_3PO_4/TNTAs sample (Figure 2(c)), a similar nanotube array structure was maintained, but many nanoparticles were observed on the surface of nanotube array (Figure 2(d)), which should be Ag_3PO_4 nanoparticles deposited on the surface of TNTAs. The FESEM result confirms that Ag_3PO_4 nanoparticles were successfully loaded onto the TNTAs. In order to further reveal the microstructure of Ag_3PO_4/TNTAs, TEM measurements were carried out on the Ag_3PO_4/TNTAs sample, and the results are shown in Figure 3. As can be seen, a large number of Ag_3PO_4 nanoparticles were evenly distributed on the surface of nanotubes with a particle size of about 2-8 nm, indicating that the Ag_3PO_4 nanoparticles could be effectively deposited on the surface of TNTAs. The TEM results further confirm the successful preparation of Ag_3PO_4/TNTAs.

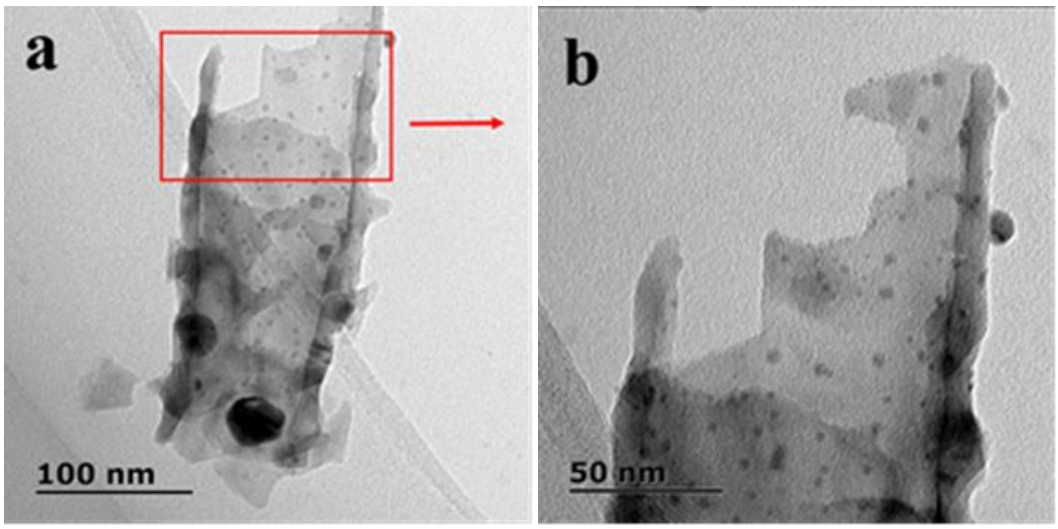

Figure 3. TEM images of the prepared Ag_3PO_4/TNTAs: (a) low magnification; (b) high magnification.

Figure 4 shows the UV-vis absorption spectra of the prepared TNTAs and Ag_3PO_4/TNTAs samples. As shown, the spectral absorption range of TNTAs was mainly in the ultraviolet region, and the visible light absorption of TNTAs was not obvious, as determined by the intrinsic semiconductor characteristics of TNTAs [28], which was in accordance with the E_g of anatase TiO_2 (E_g = 3.2 eV) [12]. For the Ag_3PO_4/TNTAs sample, the absorption in ultraviolet region remained basically unchanged, indicating that the composite had a main structure of TNTAs. Meanwhile, the visible light absorption of the Ag_3PO_4/TNTAs was significantly enhanced in comparison with TNTAs. Apparently, the enhanced visible light absorption ability of the composite could be attributed to the Ag_3PO_4 nanoparticles deposited on the surface of TNTAs, since Ag_3PO_4 has been proven to have strong visible light absorption property [29-31]. The UV-vis absorption result indicates that the loading of Ag_3PO_4 nanoparticles could

significantly affect the UV-vis light absorption of TNTAs and improve the light utilization rate of TNTAs to a large extent, thus probably leading to the enhancement of photocatalytic activity.

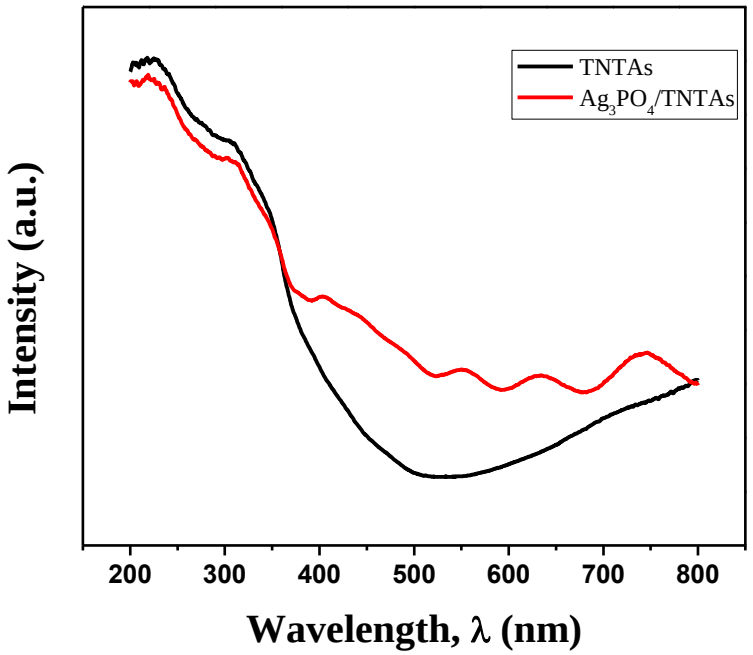

Figure 4. UV-vis absorption spectra of the prepared TNTAs and Ag3PO4/TNTAs samples.

3.2 Photocatalytic performance

The photocatalytic properties of the prepared TNTAs and Ag_3PO_4/TNTAs samples were evaluated by photocatalytic degradation of RhB. Figure 5 shows the photocatalytic degradation of RhB over the prepared TNTAs and Ag_3PO_4/TNTAs samples.

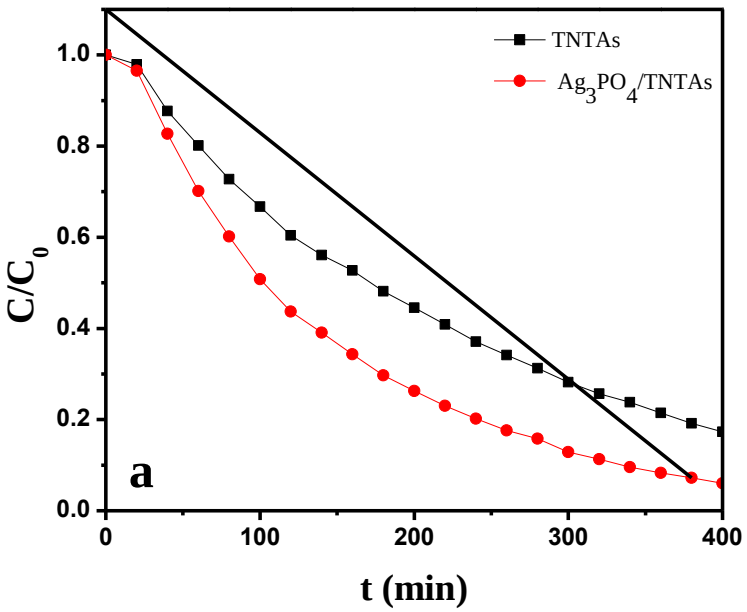

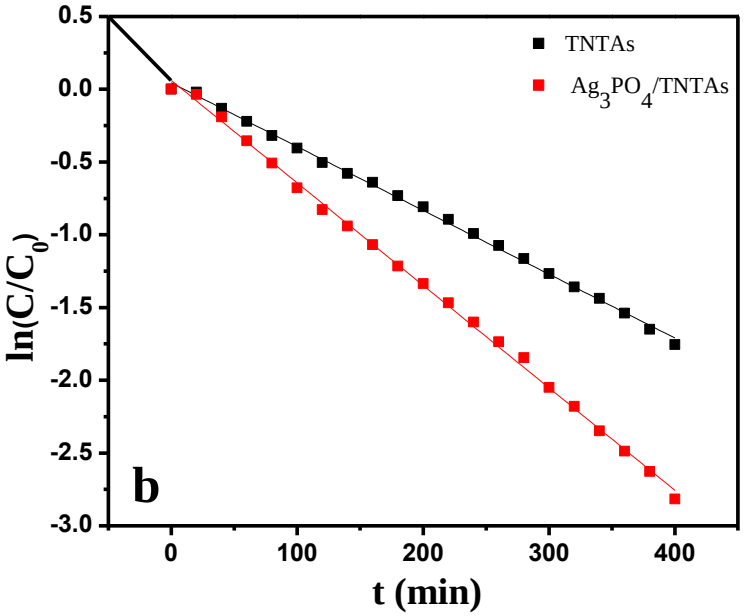

Figure 5. (a) Photocatalytic degradation efficiency of RhB over the prepared TNTAs and Ag_3PO_4/TNTAs under visible-light ($\lambda \geq 420$ nm) irradiation; and (b) the corresponding pseudo-first-order kinetics fitting data for RhB photodegradation.

As can be seen from Figure 5(a), both the TNTAs and Ag_3PO_4/TNTAs samples exhibited superior photocatalytic properties under visible light. In comparison, the photocatalytic activity of Ag_3PO_4/TNTAs was significantly higher than that of the TNTAs. In addition, the kinetic process of photocatalytic degradation of RhB conforms to the quasi-first-order rate law equation [32, 33]: $-[\ln(C/C_0)] = K_{app}t$, where K_{app} is the apparent degradation rate constant.

According to the equation, the corresponding pseudo-first-order kinetics fitting data for RhB photodegradation over the prepared TNTAs and Ag_3PO_4/TNTAs samples were presented in Figure 5(b). From Figure 5(b), the degradation rate constants (K_{app}) of the prepared TNTAs and Ag_3PO_4/TNTAs samples were calculated to be 7.64×10^{-4} min^{-1} and 1.96×10^{-3} min^{-1}, respectively, and the K_{app} of the Ag_3PO_4/TNTAs sample was about 2.6 times that of TNTAs. This indicates that the photocatalytic activity of TNTAs was significantly improved after Ag_3PO_4 nanoparticles were deposited. In our opinion, the loading of Ag_3PO_4 nanoparticles greatly improved the visible light absorption capacity and spectral utilization efficiency of TNTAs, and the heterojunction structure formed by the two also promoted the separation of photogenerated charges, which has been also demonstrated in previous work [29, 34], thus enhancing the photocatalytic activity of TNTAs to a large extent.

4. CONCLUSION

In this work, the Ag_3PO_4/TNTAs composite photocatalysts were successfully prepared by the deposition of Ag_3PO_4 nanoparticles onto the surface of TNTAs through a facile chemical impregnation method, as confirmed by XRD, FESEM and TEM measurements. The UV-vis absorption spectra reveal

that the loading of Ag_3PO_4 nanoparticles greatly improved the visible light absorption ability and spectral utilization efficiency of TNTAs. More importantly, the photocatalytic activity of Ag_3PO_4/TNTAs for RhB photodegradation was greatly improved compared with that of TNTAs, and the photocatalytic degradation rate constant (K_{app}) of Ag_3PO_4/TNTAs was about 2.6 times that of TNTAs. The improved photocatalytic performance of Ag_3PO_4/TNTAs could be attributed to the fact that Ag_3PO_4 nanoparticles could not only improve the spectral absorption ability of TNTAs but also facilitate the photogenerated charge separation efficiencies induced by the heterojunction formed between Ag_3PO_4 and TNTAs.

ACKNOWLEDGEMENT
This work was financially supported by the Scientific Research Project of Zhejiang Provincial Department of Education (No. Y201636705, Y201328116), National Key Research and Development Program of China (No. 2017YFF0204701), Zhejiang Provincial Natural Science Foundation of China (No. LY19E020003).

References

1. O. Lefebvre and R. Moletta, *Water Res.*, 40 (2006) 3671.
2. E.M. Dias and C. Petit, *J. Mater. Chem. A*, 3 (2015) 22484.
3. J. Wang, Z.J. Wang, C.L.Z. Vieira, J.M. Wolfson, G.Y. Pingtian and S.D. Huang, *Ultrason. Sonochem.*, 55 (2019) 273.
4. K. Kabra, R. Chaudhary and R. L. Sawhney, *Ind. Eng. Chem. Res.*, 43 (2004) 7683.
5. L.V. Bora and R.K. Mewada, *Renew. Sustain. Energy Rev.*, 76 (2017) 1393.
6. D.J. Chen, Y.L. Cheng, N. Zhou, P. Chen, Y.P. Wang, K. Li, S.H. Huo, P.F. Cheng, P. Peng, R.C. Zhang, L. Wang, H. Liu, Y.H. Liu and R. Ruan, *J. Cleaner Prod.*, 268 (2020) 121725.
7. B.J. Han, X.Y. Wei and R.Z. Gu, *Int. J. Electrochem. Sci.*, 16 (2021) 210618.
8. M. Pelaez, N.T. Nolan, S.C. Pillai, M.K. Seery, P. Falaras, A.G. Kontos, P.S.M. Dunlop, J.W.J. Hamilton, J.A. Byrne, K. O'Shea, M.H. Entezari and D.D. Dionysiou, *Appl. Catal. B-Environ.*, 125 (2012) 331.
9. S.K. Loeb, P.J.J. Alvarez, J.A. Brame, E.L. Cates, W. Choi, J. Crittenden, D.D. Dionysiou, Q.L. Li, G. Li-Puma, X. Quan, D. L. Sedlak, T. D. Waite, P. Westerhoff and J. H. Kim, *Environ. Sci. Technol.*, 53 (2019) 2937.
10. D. Gong, C.A. Grimes, O.K. Varghese, W.C. Hu, R.S. Singh, Z. Chen and E.C. Dickey, *J. Mater. Res.*, 16 (2001) 3331.
11. X.H. Li, G.Y. Chen, L.B. Yang, Z. Jin and J.H. Liu, *Adv. Funct. Mater.*, 20 (2010) 2815.
12. A.E. Mohamed and S. Rohani, *Energy Environ. Sci.*, 4 (2011) 1065.
13. Q.L. Huang, T. Gao, F. Niu, D. Chen, Z. Chen, L.S. Qin, X.G. Sun, Y.X. Huang and K.Y. Shu, *Superlatt. Microstruct.*, 75 (2014) 890.
14. Z.X. Xu, D. Chen, Q.L. Huang, W.L. Song, J.H. Liang, L.S. Qin and Y.X. Huang, *Int. J. Electrochem. Sci.*, 15 (2020) 5220.
15. J. Gomes, J. Lincho, E. Domingues, M. Gmurek, P. Mazierski, A. Zaleska-Medynska, T. Klimczuk, R.M. Quinta-Ferreira and R.C. Martins, *Sci. Total Environ.*, 689 (2019) 79.
16. Q.X. Zhou, Z. Fang, J. Li and M.Y. Wang, *Micropor. Mesopor. Mater.*, 202 (2015) 22.
17. M.D. Ye, J.J. Gong, Y.K. Lai, C.J. Lin and Z.Q. Lin, *J. Am. Chem. Soc.*, 134 (2012) 15720.
18. Z.G. Yi, J.H. Ye, N. Kikugawa, T. Kako, S.X. Ouyang, H. Stuart-Williams, H. Yang, J.Y. Cao, W.J. Luo, Z.S. Li, Y. Liu and R.L. Withers, *Nat. Mater.*, 9 (2010) 559.
19. Y.P. Bi, S.X. Ouyang, N. Umezawa, J.Y. Cao and J.H. Ye, *J. Am. Chem. Soc.*, 17 (2011) 6490.
20. J.H. Tan, J.H. Peng, Z. Li, D.D. Liu and W.B. Li, *Int. J. Electrochem. Sci.*, 16 (2021) 210744.

21. H. Wang, Y.S. Bai, J.T. Yang, X.F. Lang, J.H. Li and L. Guo, *Chem.-Eur. J.*, 18 (2012) 5524.
22. X.J. Chen, Y.Z. Dai and X.Y. Wang, *J. Alloy Compd*., 649 (2015) 910.
23. Z.C. Lian, W.C. Wang, S.N. Xiao, X. Li, Y.Y. Cui, D.Q. Zhang, G.S. Li and H.X. Li, *Sci. Rep*., 5 (2015) 10461.
24. T.J. Yan, J. Tian, W.F. Guan, Z. Qiao, W.J. Li, J.M. You and B.B. Huang, *Appl. Catal. B: Environ.*, 202 (2017) 84.
25. Y. Fu and A.C. Mo, *Nanoscale Res. Lett.*, 13 (2018) 187.
26. Y.Y. Feng, H.H.M. Rijnaarts, D. Yntema, Z.J. Gong, D.D. Dionysiou, Z.R. Cao, S.Y. Miao, Y.L. Chen, Y. Ye and Y.H. Wang, *Water Res.*, 186 (2020) 116327.
27. E. Montakhab, F. Rashchi and S. Sheibani, *Appl. Surf. Sci.*, 534 (2020) 147581.
28. Y.F. Zhu, *Int. J. Electrochem. Sci.*, 16 (2021) 210662.
29. Z.W. Tong, D. Yang, Y.Y. Sun, Y. Tian and Z.Y. Jiang, *Phys. Chem. Chem. Phys.*, 17 (2015) 12199.
30. R.K. Santos, T.A. Martins, G.N. Silva, M.V.S. Conceição, I.C. Nogueira, E. Longo and G. Botelho, *ACS Omega*, 5 (2020) 21651.
31. G.N. Silva, T.A. Martins, I.C. Nogueira, R.K. Santos, M.S. Li, E. Longo and G. Botelho, *Mater. Sci. Semicond. Process.*, 135 (2021) 106064.
32. L. Shi, D. Chen, W.T. Xie, J. Zhang, G.X. Ping, M.Q. Fan, L.S. Qin, L.Q. Bai, Z. Chen, C.J. Lv and K.Y. Shu, *Nano*, 11 (2016) 1650001.
33. M.F. Guo, Z.B. Zhou, S.N. Yan, P.F. Zhou, F. Miao, S.J. Liang, J.L. Wang and X.Y. Cui, *Sci. Rep.*, 10 (2020) 18401.
34. E. Nyankson, J.K. Efavi, B. Agyei-Tuffour and G. Manu, *RSC Adv.*, 11 (2021) 17032.